

A Study of Thermal Cycling and Radiation Effects on Indium and Solder Bump Bonds

S. Kwan, J. A. Appel, G. Chiodini, D. Christian, S. Cihangir and F. Reygadas[#]

Fermi National Accelerator Laboratory^{*}

Batavia, IL 60510, USA

C. Newsom

The University of Iowa

Iowa City, IA 52242, USA

Abstract-- The BTeV hybrid pixel detector is constructed of readout chips and sensor arrays which are developed separately. The detector is assembled by flip-chip mating of the two parts. This method requires the availability of highly reliable, reasonably low cost fine-pitch flip-chip attachment technology. We have tested the quality of two bump-bonding technologies; indium bumps (by Advanced Interconnect Technology Ltd. (AIT) of Hong Kong) and fluxless solder bumps (by MCNC in North Carolina, USA). The results have been presented elsewhere [1]. In this paper we describe tests we performed to further evaluate these technologies. We subjected 15 indium bump-bonded and 15 fluxless solder bump-bonded dummy detectors through a thermal cycle and then a dose of radiation to observe the effects of cooling, heating and radiation on bump-bonds. We also exercised the processes of HDI mounting and wire bonding to some of the dummy detectors to see the effect of these processes on bump bonds.

technologies had low failure rates ($\sim 10^{-4}$ failure/bump) and 1-2 Ohms bump resistance. We also established the importance of proper manufacturing procedures such as alignment, removal of oxide on the aluminium pads and having a clean environment.

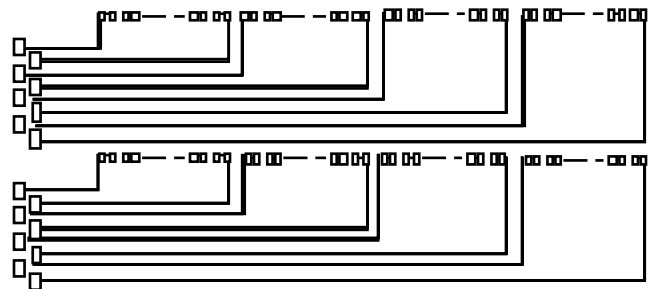


Fig. 1. AIT Dummy Detector Bump Daisy Chain.

I. TESTED COMPONENTS

THE dummy detectors were single flip-chip assemblies of daisy-chained bumps. Measured channels were composed of 30 micrometer pitch indium bumps, a chain of 28 to 32; and 50 micrometer pitch solder bumps, a chain of 14 to 16. Fig. 1 shows a schematic layout of a portion (8 channels) of an AIT dummy detector. A scanning electron micrograph of indium bumps on two pads is shown in Fig. 2 and that of a cross section of a solder a bump-bonded assembly is shown in Fig. 3. Each chain was connected to pads on each end over which we measured the resistance to characterize the channel. AIT detectors had 200 channels each; and the MCNC detectors had 190 channels each. We reported earlier [1] that both indium and solder bump

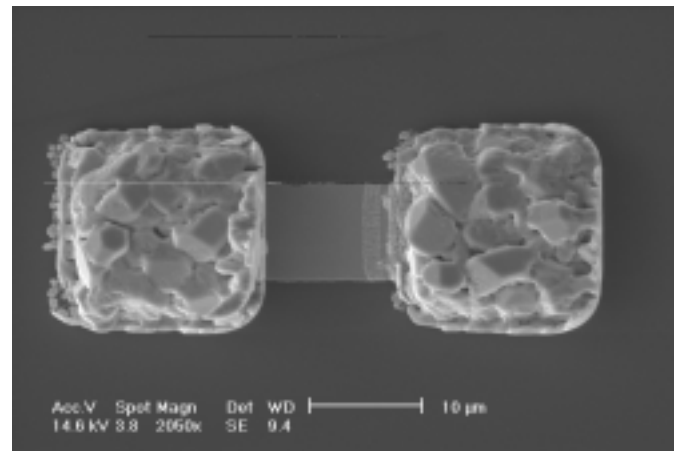


Fig. 2. AIT Dummy Detector Indium Bumps.

[#] Work made possible by the Leon Lederman Award granted by the Hertells Foundation.

^{*} Work supported by U. S. Department of Energy under contract no. DE-AC02-76CH0300.

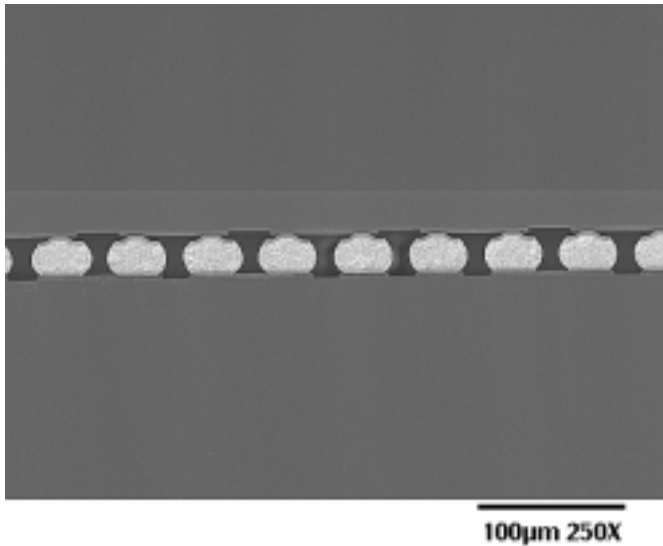


Fig. 3. MCNC Dummy Detector Solder Bump Daisy Chain.

II. THERMAL CYCLING AND RADIATION

Each detector was measured first for continuity before thermal cycling and radiation. These measurements were compared to the electrical resistance measurements done about 12 months ago[1] to yield an understanding of “time effect” on the bump-bonds. Then they were cooled to -10°C in a freezer in an air tight container for 144 hours. Subsequent measurements were compared to the measurements done before cooling to understand any “cooling effect” on the bump-bonds. This was followed by heating the detectors to 100°C in vacuum for 48 hours. The detectors were measured after heating and compared to the measurements done after cooling to yield an understanding of any “heating effect”. Finally, the dummy detectors were shipped to the University of Iowa in three shipments to be radiated by a Cs-137 gamma source to 13 MRad and measured again to understand any “radiation effect”. A randomly selected sample of detectors in each shipment was not radiated to give us an indication if the detectors were affected during shipment. This way we eliminated one of the shipments from consideration.

III. RESULTS

We reported some of the results elsewhere [2]. Here we report additional results obtained since then along with the original results.

The effects we studied manifested themselves as large increases in resistance on the channels measured. These occurrences are categorized for both types of bumps and are described below.

A. Thermal Cycling

We categorize the problem occurrences after each step of the thermal cycling as follows:

1. Indium Bumps:

Occurrence A: A good channel (1-2 Ohms average resistance per bump) develops a high resistance (5-10 KOhms per bump) in 12 months.

Occurrence B: A good channel develops a high resistance after cooling.

Occurrence C: A good channel develops a high resistance after heating.

In most cases the high resistance is accompanied by an average capacitance per bump of 2-10 picofarads.

2. Solder Bumps:

Occurrence A: A good channel (1-2 Ohms average resistance per bump) is broken (a resistance of larger than 20 MOhms) in 12 months.

Occurrence B: Cooling breaks a good channel.

Occurrence C: Heating breaks a good channel.

Table I shows the distribution of the occurrences in indium bump detectors. No entry means no problem. The last column indicates the number of channels having an open or high resistance problem before the thermal cycling. There is a correlation between the occurrences of new problems and the original existence of problems. For instance, detectors E11 and E20 which originally had many problematic channels developed more new problematic channels over the thermal cycling.

TABLE I
INDIUM BUMP PROBLEM OCCURRENCE DISTRIBUTION

Det-ID	Occur-A	Occur-B	Occur-C	Orig-Bad
E2				
E3			1	
E4				
E5				1
E8				
E11	14		1	37
E13	1		6	
E14	2			
E15			2	4
E16				
E20	20	2	8	74
E22				
E23			1	
E24				
E25				

Table II shows the distribution of the occurrences in solder bump detectors. No entry means no problem. The last column indicates the number of channels having a problem before the thermal cycling. Here we also see a correlation between the occurrences of new problems and the existence of problems before the thermal cycling. For instance, detectors MCNC-24 and MCNC-27 which originally had

many problematic channels developed more new problematic channels over the thermal cycling.

TABLE II
SOLDER BUMP PROBLEM OCCURRENCE DISTRIBUTION

Det-ID	Occur-A	Occur-B	Occur-C	Orig-Bad
MCNC-10	7	1	1	
MCNC-11				
MCNC-12				
MCNC-18				
MCNC-19				
MCNC-24	6	3	6	5
MCNC-27		1	7	12
MCNC-44				1
MCNC-50			1	1
MCNC-55			4	2
MCNC-59				1
MCNC-75				
MCNC-76			3	
MCNC-81				
MCNC-86	4	1	5	3

We calculated the occurrences per bump based on these observations and summarize the results in Table III. The correlation mentioned above can be a reason to exclude detectors E11, E20, MCNC-24 and MCNC-27 from consideration for the effects of thermal cycling. If we do that, we then calculate the occurrence rates per bump as shown in Table IV.

TABLE III
RATE OF OCCURRENCES (PER BUMP)

Occurrence	Indium Bumps	Solder Bumps
A	2.1×10^{-4}	4.0×10^{-4}
B	2.2×10^{-5}	1.4×10^{-4}
C	2.1×10^{-4}	6.3×10^{-4}

TABLE VI
RATE OF OCCURRENCES (PER BUMP) WITHOUT PROBLEMATIC DETECTORS

Occurrence	Indium Bumps	Solder Bumps
A	3.3×10^{-5}	2.6×10^{-4}
B	2.2×10^{-5}	4.6×10^{-5}
C	2.5×10^{-5}	3.3×10^{-4}

B. Radiation

On indium bump detectors, after the radiation we observed that almost every first channel in groups of four channels (see Fig. 1) was at high resistance. The group of four channels is a geometrical pattern of the construction of these detectors. To further investigate the situation, we took

apart a flip-chip assembly dummy detector and heated the bottom part. This detector was not heated or radiated before. We noticed that the indium diffused over all gold strip lines (Fig. 4). A closer view is shown in Fig. 5. Additional heating caused the indium diffuse even more, proportionally to temperature and heating time. We also noticed that the diffusion was present at every channel on all heated detectors, but they were darker in color on every fourth channel on heated and radiated detectors. Those are the channels that have high resistance and geometrically they are located at the edge of the detectors.

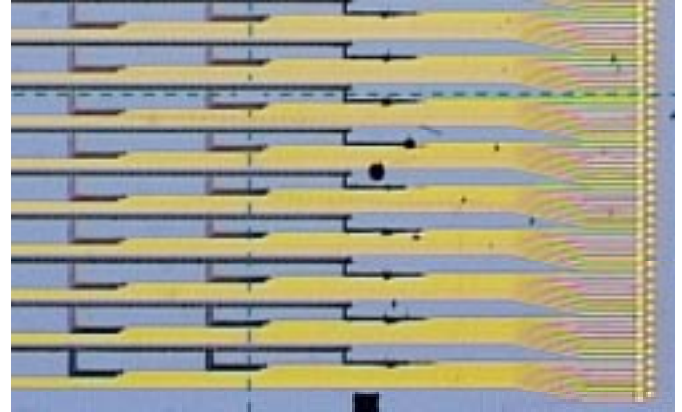


Fig. 4. Indium diffusion (dark lines) onto gold strips.

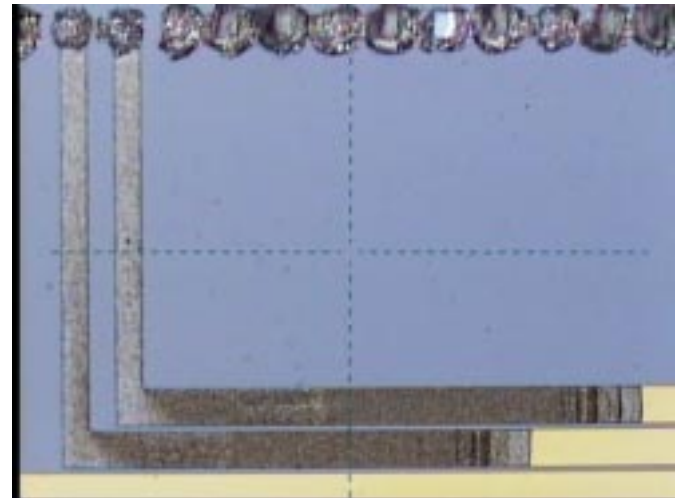


Fig. 5. Indium diffusion onto gold strips, closer view.

A possible explanation is as follows: Indium diffuses with heat onto gold strips and the rate increases with rising temperature. Naturally occurring oxidization on indium is accelerated by radiation. Oxidized bump joints then cause the high resistance. Oxidization is more effective on the edge of the detectors since oxygen is readily available there compared to the inner area for which the air circulation is restricted by mesh of bumps.

We should point out that this effect will not be present in real detectors for two reasons: 1) Aluminium will be used in

real detectors instead of gold and we did not observe indium diffusion onto aluminium strips. 2) No passivation was used on dummy detectors in order to save money. Passivation would prevent the indium from being in contact with the metal lines and therefore block the diffusion process.

On solder bump detectors, we observed that the aluminium layers both on the strips and the pads were extensively flaky and bubbly after the radiation as seen in Fig. 6. This may be a result of accelerated oxidation with radiation. We observed 6 out of 2280 channels (each with 14 or 16 bumps) were broken. This indicates a rate per bump of 1.8×10^{-4} for the radiation effect. We should point out that these 6 failures might be due to breakage in the aluminium strips due to radiation rather than the breakage on the bump-bonds. We can not distinguish this effect at the present time for geometrical and structural reasons, but will investigate in the future.

Three solder bump detectors were radiated to additional 17 MRad. Six out of 570 channels were broken yielding a rate per bump of 7.0×10^{-4} at this dose.



Fig.6. Formation of flakes on Al pads and strips after radiation.

IV. HDI MOUNTING

We mounted and wire bonded prototype HDI's (High Density Interconnects) onto some of the dummy detectors to see the effect of these processes on the bump bonds. The base material of the HDI's was kapton and they were mounted using NEE-001 or DP-110 epoxies. The rates for broken bumps after HDI mounting and wire bonding were 2.3×10^{-5} and 7.6×10^{-5} per bump, respectively. We afterwards cooled them to -10°C for seven days and heated to 50°C for three hours to study the effect of mechanical stress due to expansion or contraction caused by thermal cycling. The failure rate per bump for thermal cycling effect was 3.8×10^{-4} .

V. CONCLUSIONS

The results of thermal cycling and radiation tests validate the feasibility of bump-bonding technologies for hybrid pixel detectors. They withstand extreme conditions. Heating to 100°C , though, is more destructive than cooling to -10°C , while the radiation effect is minimal. There is a correlation between the occurrences of problems due to these effects and existence of problems when the detectors were first assembled. The rates quoted are probably inflated due to the fact that some failures are caused by damage to the strips and pads due to repeated probing and radiation. Mechanical stress created on the detectors by mounting and wire bonding the HDI's had very small effect on the bump bonds. The cooling and heating effects after HDI mounting were similar to the effects observed before mounting.

VI. REFERENCES

- [1] S. Cihangir and S. Kwan, "Characterization of Indium and Solder Bump Bonding for Pixel Detectors", talk presented at the 3rd International Conference on Radiation Effects on Semiconductor Materials, Detectors and Devices, Florence, Italy (June 28-30, 2000), to appear in Nuclear Instruments and Methods A. Also Fermilab preprint FERMILAB-Conf-00/168-E.
- [2] S. Cihangir et al., "A Study of Thermal Cycling and Radiation Effects on Indium and Solder Bump Bonding", talk presented at the 7th Workshop on Electronics for LHC Experiments, Stockholm, Sweden, Sept. 10-14. Also, Fermilab preprint FERMILAB-Conf-01/251-E.